


RESEARCH

Open Access



Multiparametric magnetic resonance imaging in the assessment of pathological axillary lymph nodes in cases of breast cancer

Rania Mohamed Abbas Hegazy^{1*} , Shereen Mohamed AbdelRaouf Khalil¹, Sherif Mohamed Mokhtar² and Fatma Mohamed AbdelRahman Awad¹

Abstract

Background Breast cancer is the most frequent cancer affecting females. It represents leading cause of death from all cancers in females. Traditionally, axillary staging was surgically assessed by axillary lymph node dissection (ALND), which is associated with complications. Sentinel lymph node biopsy (SLNB) is a minimally invasive surgical method for axillary staging in patients with primary breast cancer with lower morbidity and better quality of life. Clinical examination of the axilla is usually associated with a high false negative rate, so role of imaging is crucial to identify lymph nodes with or without suspicious features, to predict the pathological state of the lymph nodes and to direct the diagnostic and therapeutic process toward SLNB, ALND, or chemotherapy. Aim of this study was to assess axillary lymph nodes in breast cancer patients by magnetic resonance imaging and functional MRI preoperatively to determine its nature and eliminate invasive procedures as invasive dissection used in diagnosis.

Results Lymph node size cannot significantly predict malignant infiltration with p value 0.425, using cut-off value of 21.5 mm, with a sensitivity of 14.6% and specificity of 100%. Cortical thickness of lymph nodes can significantly predict malignant infiltration with p value 0.006, using cut-off value of 4.5 mm, with a sensitivity of 68.8%, specificity of 62.5%, and diagnostic accuracy of 64.1%. ADC can significantly predict lymph node infiltration with p value 0.011, using a cut-off value of 0.99, with sensitivity of 43.85, specificity of 100%, diagnostic accuracy of 57.8%, and AUC of 71.4%. There was a statistically significant correlation between pathological findings and DCE-MRI curve type III with p value 0.0001, showing a sensitivity of 37.5%, specificity of 100%, and diagnostic accuracy of 84.4% for detection of malignant lymph nodes.

Conclusions Cortical thickness and effaced fatty hilum of lymph nodes can significantly predict malignant infiltration, while lymph node size cannot significantly predict malignant infiltration. Diffusion weighted images and ADC maps can be of significant value in predicting metastatic lymph nodes with approximate ADC cut-off value of 0.99. Kinetic MRI features of the axillary lymph nodes are not reliable enough to be used alone in the clinical management of breast cancer patients.

Keywords Breast cancer, Multiparametric MRI, Axillary lymph nodes

*Correspondence:

Rania Mohamed Abbas Hegazy
raniahegazy@hotmail.com; hegazyrania@gmail.com

¹ Diagnostic and Interventional Radiology Department, Faculty of Medicine, Cairo University, Cairo, Egypt

² General Surgery Department, Faculty of Medicine, Cairo University, Cairo, Egypt

Background

Breast MRI is useful in evaluation of breast cancer tumor extent and in assessing treatment response following neoadjuvant chemotherapy as well. The advantage of MRI over US is that MRI gives a more global view of both axillae, increasing the detection of potentially

abnormal LNs as well as allowing comparison of the axillae irrespective to the patient body habitus. Also, it is less operator-dependent and more objective than US. So, it is important to include the axillary regions in breast MRI examinations [1, 2].

Diffusion-weighted (DW) MRI is a valuable MRI sequence that does not need IV contrast injection. It showed promising results in differentiating benign from malignant breast lesions in a relatively short imaging acquisition time. DW MRI has sensitivity to tissue characteristics as membrane integrity, cell density, and microstructure, so it might give information complementary to that obtained with dynamic contrast enhanced MRI (DCE-MRI). Recent studies of breast DW MRI showed that the apparent diffusion coefficient (ADC) was significantly lower in malignant breast lesions compared to benign lesions and normal tissues. Recent several studies showed variable specificities (77–91%) and sensitivities (53.8–94%) of DW MRI for axillary lymph node metastases [3].

Although MR imaging allows for the analysis of both axillae, morphological analysis is limited compared to ultrasound, as the main criteria as round shape and intracortical nodule are rather not specific [4, 5]. Yet, irregular cortical thickening, loss of hilum, irregular edges, and asymmetry in number and/or size of lymph nodes compared to contralateral axilla present some useful MR imaging criteria that help to detect nodal invasion [4, 5] MR imaging is also effective in detecting perinodal edema signal that can be easily seen on T2WIs as well as the more important invasions with a ring-like enhancement representing central necrosis [5, 6]. Similarly, DW MR images using high b-values (750–1200 s/mm²) are useful in detection of metastatic lymph nodes, especially those on the limits of the field of view, which must be confirmed whether or not they are pathological by analyzing the conventional images as (T1- and T2-weighted sequences) [7]. ADC measurement could also be useful in characterizing pathological nodes. An ADC value less than 1×10^{-3} mm²/s is considered pathological [5, 8]. Several studies have found that performing ultrasound-guided FNA in lymph nodes with normal morphology on ultrasonography could increase sensitivity in detecting metastases, particularly in patients with larger tumors. However, US-guided FNA is an invasive method to diagnose metastases. In addition, its sensitivity is relatively low (39.5–86%), yet its specificity is high (95–100%) [9, 10].

Magnetic resonance imaging can be used in determination of axillary lymph nodes status with the added benefits of giving a global view of both axillae regardless of the patient's habitus as well as the functional analysis of both the breast lesion and lymph nodes [1]. Imaging

still plays a very important role in guiding axillary lymph node excision or SLNB. MRI aims to minimize intervention while preserving or even enhancing the patient outcome [1].

Aim of this study was to assess axillary lymph nodes in breast cancer patients by magnetic resonance imaging and functional MRI preoperatively to determine its nature and eliminate invasive procedures as invasive dissection used in diagnosis.

Methods

This is a prospective study that included 64 females during the period from April 2021 to July 2022. The age of the patients ranged from 34 to 76 years (mean age 52.7 ± 10.1 SD). Patients with pathologically proven breast cancer having indeterminate or infiltrated lymph nodes were targeted by our study. They presented to the General Surgery Department at our general hospital with variable complaints, including breast lump and axillary lumps. The patients underwent full history taking and clinical examination then were referred to the female imaging unit in the radiology department, for full field digital mammography, ultrasound, and biopsy.

The selected patients then had dynamic contrast-enhanced MRI of both breasts done for them. This study was conducted after institutional and departmental ethical clearance and informed consent was obtained from patients or their authorized representatives. Ethics committee code: MD-94-2021.

Inclusion criteria

All patients with histopathologically proven breast cancer, who did digital mammography and breast ultrasound and had pathological (indeterminate or infiltrated) lymph node in ultrasound study and who had no contraindication to MRI, were included in our study.

Exclusion criteria

Patients with benign breast masses or patients lost to histopathology were excluded from the study. Patients who had a contraindication to MRI, e.g., implanted cardiac pacemaker, cochlear implant, or a contraindication to MRI contrast material (renal impairment, allergic patients, or those known to have history of anaphylactic reaction from contrast media). Patients with normal breast study or proven cases of breast cancer yet absent axillary lymph nodes were also excluded from the study. A flowchart has been plotted showing how the patient population was selected during the current study (Fig. 1).

All patients were submitted to the following 1. Demographic and clinical data collection, including patient's name, age, marital status, residence, and diagnosis. 2. Imaging procedure: All patients underwent post-contrast

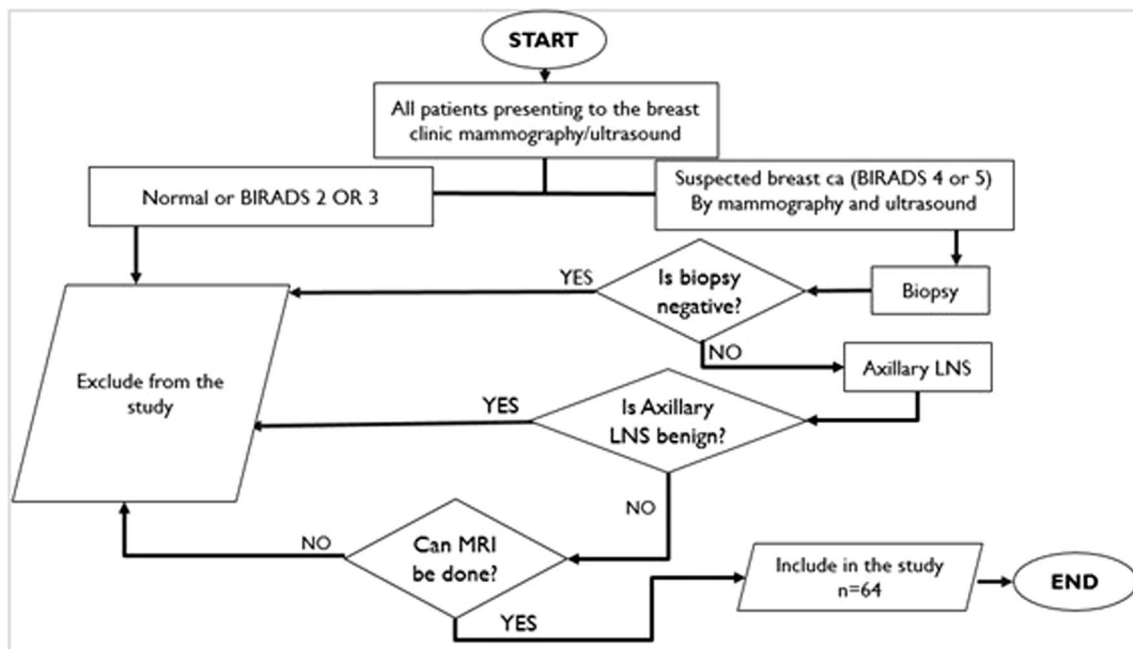


Fig. 1 Flowchart showing patient selection

MRI and ultrasound examination of breast and axilla. MRI protocol and ADC value calculation: *MRI Protocol Equipment* The study was conducted on 1.5 Tesla MRI machine (Philips Achieva and Intera, Amsterdam, Netherlands). *Patient Preparation* The patient was asked to empty the urinary bladder prior to the study. A cannula was applied in an antecubital vein for contrast injection. The catheter was then tested with small amount of manual saline injection to ensure adequate positioning and patency. The patient then lied prone on the MRI table, and both breasts were inserted into a dedicated double-breast coil. *Image Acquisition* Includes the standard MR protocol for breast MR, Diffusion sequences and DCE-MRI. This is followed by post-processing of the images. *Standard MRI Protocol* Three plane localizers were initially obtained to localize and plan the sequences using fast single-shot localizers. Axial T1WI was obtained with the spin echo sequence with the following parameters: repetition time/echo time: 10 ms/5 ms; number of excitations: 2; direction of frequency encoding: R/L; section thickness: 3 mm; gap: 0.5 mm; field of view: 36–40 cm; and matrix: 288×224. Axial T2 and Axial and Sagittal STIR were obtained with the following parameters: repetition time/echo time, 1.6 ms/20 ms; number of excitations, 3; direction of frequency encoding: R/L; section thickness, 3 mm; gap, 1 mm; field of view, 36–40 cm; and matrix, 288×224. *Diffusion-Weighted (DW) MRI Protocol* DW-MRI technique was performed using single-shot echo planar imaging together with fat suppression. The

following parameters were used; 5000 ms/75 ms (repetition time/echo time), 5 mm (section thickness), 256×256 (matrix), 30×30 cm (field of view), and 3 mm (section gap). Regarding b-value in our study, three b-values were used; 0, 500, and 1000 s/mm². The apparent diffusion coefficient (ADC) maps were calculated by the MR system via linear regression analysis of the natural log of signal intensity using all b-values. *Dynamic contrast-enhanced (DCE) MRI Protocol* Six dynamic acquisitions, one before and 5 after intravenous injection of contrast, with and without subtraction, were obtained in the axial plane. Contrast medium used was 0.1 mmol/kg body weight of Gadolinium-diethylenetriamine penta-acetic acid; Gd-DTPA, injected manually at a rate of 2 ml/s and using the dynamic THRIVE sequence (T1 high-resolution isotropic volumetric examination) (TR/TE = 5/2 ms) in 1.6-mm slice thickness. *Post-processing: Choice of Targeted Lymph Nodes* Lymph nodes were targeted by their side and level obtained on ultrasound aided by their morphology on T1WIs; if the lymph node cannot be identified, then the closest lymph node to the lesion (sentinel lymph node) was selected. If multiple lymph nodes were presented in the same axilla, the largest most suspicious node was analyzed.

DW-MR imaging ADC value calculation

Signal intensity (SI) in DW images and ADC maps was recorded, and ROIs were drawn manually on the ADC map. ROIs were defined as slightly smaller than the

actual nodes in order to reduce partial volume effects. Mean ADC values were recorded. Diffusion restriction was evaluated according to the qualitative assessment (the signal pattern in DWI and ADC map). Qualitative Assessment: Visual assessment of signal intensity in DW images at b 500 and 1000 and the corresponding ADC map images was determined and classified as follows: *Free diffusion* high or intermediate SI on DWI without decrease in SI on the corresponding ADC map. *Restricted diffusion* high or intermediate SI on DWI with total decrease or loss of SI on the corresponding ADC map. Quantitative Assessment: Mean ADC value was calculated by manually drawing regions of interest (ROI) in the most restricted (hypo-intense) portion of the selected LN on the ADC map. Multiple measurements were acquired, and the mean value was calculated. *DCE-MR Imaging* Dynamic curve acquisition was done by applying the ROI voxel upon the cortex of the targeted lymph node. The most malignant curve was considered for each lymph node. Acquired curves were grouped into three types: type I (rising, benign), type II (plateau, indeterminate), and type III (declining, malignant) curves. Images were interpreted by two experienced breast radiologists of 12- and 26-year experience. Interpretation was done in consensus.

Standard reference

MR Imaging findings were compared with pathological results obtained after surgery (50 cases) or after fine needle aspiration cytology (FNAC) (14 cases) of the lymph node.

Statistical analysis

Statistical analysis was conducted using SPSS 22nd edition, and quantitative data were presented in mean and standard deviation. Categorical data were presented in frequency and percentages and were compared using McNamar test. Sensitivity, specificity, NPV, PPV, and diagnostic accuracy were calculated using 2x2 contingency tables. Sensitivity analysis was conducted to assess diagnostic ability of MRI findings of axillary lymph nodes for positive malignant infiltration. Any *p* value <0.05 was considered significant.

Results

A total of 64 females were assessed using breast MRI for axillary LN infiltration by malignant cells, and they had a mean age of 52.7 years.

Demographics The age of patients included in the study ranged from 34 to 76 years with a mean age 52.7 years. Lymph Node Appearance (Table 1): MRI showed that the median lymph node size was 12 mm (range 5–60 mm) and median cortical thickness was 5 mm (range

Table 1 Lymph node appearance by imaging

Lymph node size (mm)	Median, range	12.0	5–60
Cortical thickness (mm)	Median, range	5	3–30
Fatty hilum			
Normal	N, %	40	62.5%
Eccentric hilum	N, %	24	37.5%

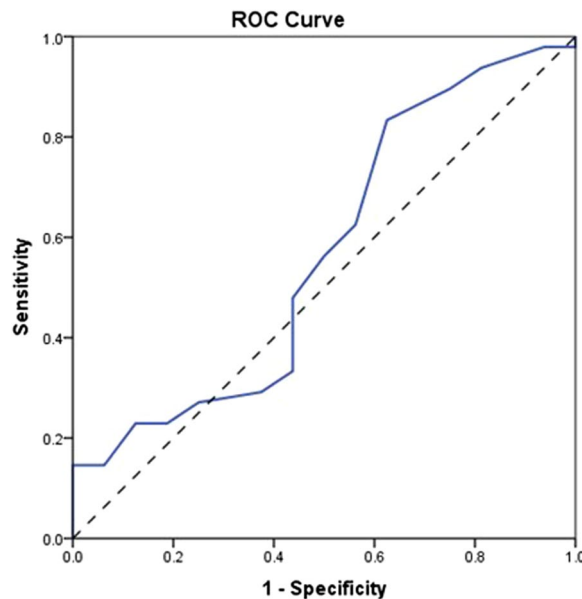


Fig. 2 ROC curve showing predictability of lymph node size for malignant infiltration

3–30 mm). Examination of fatty hilum showed eccentric allocation in 24 (37.5%) patients. Lymph node size cannot significantly predict malignant infiltration with *p* value 0.425, using cut-off value of 21.5 mm, with a sensitivity of 14.6% and specificity of 100% ((Fig. 2) and (Table 2)). However, cortical thickness of lymph nodes can significantly predict malignant infiltration with *p* value 0.006, using cut-off value of 4.5 mm, with a sensitivity of 68.8%, specificity of 62.5%, and diagnostic accuracy of 64.1%. (Fig. 3), (Table 3). There was a statistically significant difference between eccentric and normal fatty hilum status with *p* value 0.0001, with sensitivity of 47.9%, specificity of 93.7%, and diagnostic accuracy of 82.3% of eccentric hilum for detection of malignant lymph nodes (Table 4).

Pathology findings

Pathological examination showed that 48 (75%) patients had malignant lymph nodes, while 16 (25%) patients had benign lymph nodes (total 64 lesions).

Table 2 Lymph node size

AUC	p value	Diagnostic indices			
		Cut-off	Sensitivity	Specificity	95% CI
.567	.425	21.5	14.6%	100%	.395 .739

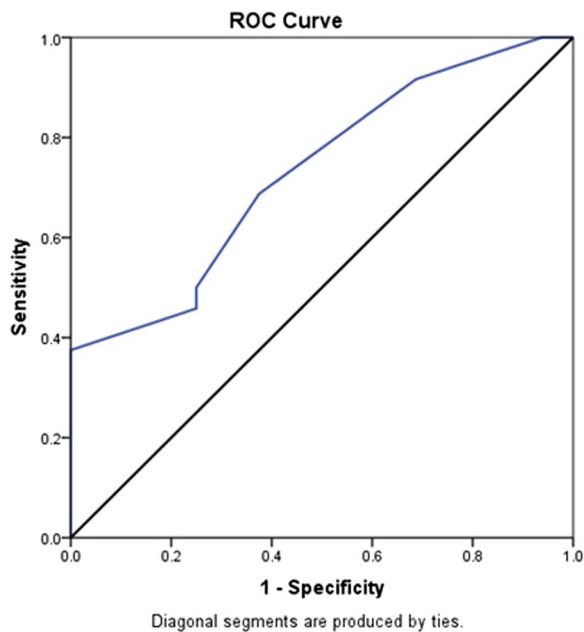


Fig. 3 ROC curve showing predictability of cortical thickness for malignant infiltration

Diagnostic indices; diffusion-weighted (DW) MRI

ADC can significantly predict lymph node infiltration with p value 0.011, using a cut-off value of 0.99, with sensitivity of 43.85, specificity of 100%, diagnostic accuracy of 57.8%, and AUC of 71.4%. (Fig. 4) (Table 5). *Dynamic contrast-enhanced (DCE) MRI* curve of DCE-MRI was type I in 19 (29.7%) patients, type II in 27 (42.2%) patients, and type III in 18 (28.1%) patients.

Comparison of pathological findings according to type of DCE-MRI curve showed that there was a statistically significant correlation between pathological findings and DCE-MRI curve type III with p value 0.0001, showing a sensitivity of 37.5%, specificity of 100%, and diagnostic

Table 3 Cortical thickness

AUC	p value	Diagnostic indices					95% CI	
		Cut-off	Sensitivity	Specificity	NPV	PPV		Accuracy
.731	.006	4.5	68.8%	62.5%	85.7%	37.9%	64.1%	.598 .864

Table 4 Fatty hilum status

	Pathology				p value
	Malignant		Benign		
	Count	Row N %	Count	Row N %	
Fatty hilum					
Normal	25	62.5	15	37.5	0.0001
Eccentric hilum	23	95.8	1	4.2	

accuracy of 84.4% for detection of malignant lymph nodes (Tables 6, 7).

Tables 8, 9, 10, 11, 12, 13 and 14 demonstrate paired comparison of combined US findings versus pathology.

Discussion

In 2020, breast cancer accounted for 24.5% of all female-diagnosed cancers [11]. Traditionally, the axillary staging was surgically assessed by axillary lymph node dissection (ALND), which is potentially associated with complications such as uncomfortable postoperative drains, seromas, cellulitis, lymphedema, range-of-motion restriction, arm paresthesia, and pain [5]. Sentinel lymph node biopsy (SLNB) is a minimally invasive surgical method for axillary staging in patients with primary breast cancer with lower morbidity and better quality of life [12]. Since clinical examination of the axillary cavity is associated with a high false negative rate, the role of imaging becomes crucial to identify lymph nodes with suspicious features, to direct the diagnostic and therapeutic process toward SLNB, ALND, or neoadjuvant chemotherapy [13]. In recent years, many noninvasive imaging modalities have been suggested for this purpose. Axillary evaluation using MRI has several advantages over other imaging modalities, such as the lack of ionizing radiation (compared to PET/CT) or less intra- and inter-observer variations (common in ultrasound examinations) [14].

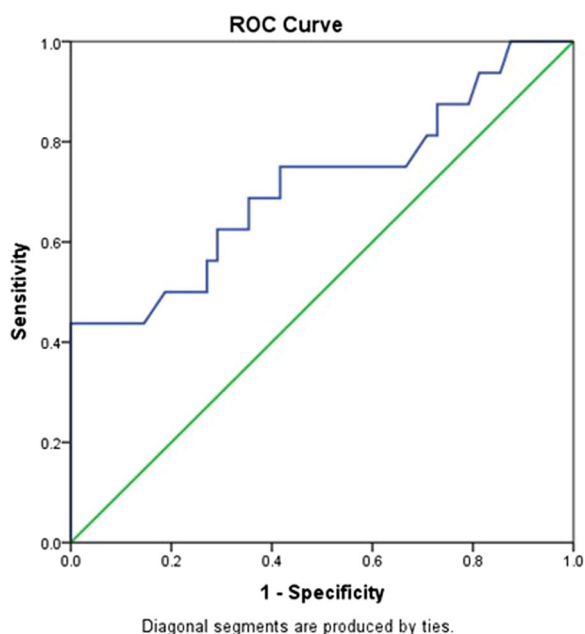


Fig. 4 ROC curve showing predictability of ADC for malignant lymph nodes

The aim of this study was to assess axillary lymph nodes in breast cancer patients by magnetic resonance imaging and functional MRI preoperatively to determine its nature and eliminate invasive procedures as invasive dissection used in diagnosis. In the current study, 64 females were assessed using breast MRI for axillary lymph node infiltration by malignant cells. These patients had a mean age of 52.7 years. Barco et al. [16] stated that 61.1% of the patients had negative nodes, while 38.9% of the patients had positive nodes, while in our study, we found that 75% of the patients had positive lymph nodes, while 25% of the patients had negative lymph nodes. In the present study, we found that MRI showed that the median lymph node size was 12 mm (range 5–60 mm) and median cortical thickness was 5 mm (range 3–30 mm). Examination of fatty hilum showed eccentric allocation in 24 (37.5%) patients. A study by Baltzer et al. [6] illustrated that the mean longest diameter of lymph nodes was 13.0 mm versus 16.5 mm in nodal positive versus nodal negative cases, whereas in our study, we found that the mean longest diameter of lymph nodes was 15.14 mm versus 13.0 mm in nodal positive versus nodal negative cases,

Table 6 DCE-MRI curve type

	Pathology				p value
	Malignant		Negative		
	Count	Row N %	Count	Row N %	
Curve type					
I	10	52.6	9	47.4	0.0001
II	20	74.1	7	25.9	
III	18	100.0	0	0.0	

Table 7 Diagnostic indices of DCE curve type III

Statistic	Value (%)	95% CI
Sensitivity	37.50	23.95–52.65%
Specificity	100.00	79.41–100.00%
Disease prevalence	25.00	
Positive predictive value	100.00	
Negative predictive value	82.76	79.40–85.67%
Accuracy	84.38	73.14–92.24%

Table 8 ADC value less than 0.99 (our calculated cut-off value) + cortical thickness 3–4 mm

Statistic	Value (%)	95% CI
Sensitivity	4.17	0.51–14.25%
Specificity	100.00	79.41–100.00%
Disease prevalence	75.00	62.60–84.98%
Positive predictive value	100.00	
Negative predictive value	25.81	24.69–26.95%
Accuracy	28.12	17.60–40.76%

respectively. In the current study, we found that lymph node size cannot significantly predict malignant infiltration, in agreement with Baltzer et al. [6] with a p value 0.425, using cut-off value of 21.5 mm, with a sensitivity of 14.6% and specificity of 100%. Kim et al. [9] who examined size, maximal cortical thickness, and ADC value showed statistically significant differences between the two groups (p value 0.001). The size was not a significant factor for predicting a metastatic axillary lymph node. Eccentric cortical thickening was found to be a

Table 5 ADC cut-off value

AUC	p value	Diagnostic indices					95% CI		
		Cut-off	Sensitivity	Specificity	NPV	PPV	Accuracy		
.714	.011	0.99	43.8%	100%	100%	37.2%	57.8%	.550	.877

Table 9 ADC value less than 0.99 (our calculated cut-off value) + cortical thickness 3–4 mm + type I dynamic curve

Statistic	Value (%)	95% CI
Sensitivity	6.25	1.31–17.20%
Specificity	87.50	61.65–98.45%
Disease prevalence	75.00	62.60–84.98%
Positive predictive value	60.00	21.55–89.12%
Negative predictive value	23.73	20.32–27.52%
Accuracy	26.56	16.30–39.09%

Table 10 ADC value less than 0.99 (our calculated cut-off value) + cortical thickness 3–4 mm + type II dynamic curve

Statistic	Value (%)	95% CI
Sensitivity	14.58	6.07–27.76%
Specificity	75.00	47.62–92.73%
Disease prevalence	75.00	62.60–84.98%
Positive predictive value	63.64	37.03–83.89%
Negative predictive value	22.64	17.73–28.44%
Accuracy	29.69	18.91–42.42%

Table 11 ADC value less than 0.99 (our calculated cut-off value) + fatty hilum + cortical thickness 3–4 mm + type III dynamic curve

Statistic	Value (%)	95% CI
Sensitivity	10.42	3.47–22.66%
Specificity	100.00	79.41–100.00%
Disease prevalence	75.00	62.60–84.98%
Positive predictive value	100.00	
Negative predictive value	27.12	25.25–29.07%
Accuracy	32.81	21.59–45.69%

Table 12 ADC value less than 0.99 (our calculated cut-off value) + fatty hilum + cortical thickness > 4 mm + type I dynamic curve

Statistic	Value (%)	95% CI
Sensitivity	14.58	6.07–27.76%
Specificity	100.00	79.41–100.00%
Disease prevalence	75.00	62.60–84.98%
Positive predictive value	100.00	
Negative predictive value	28.07	25.77–30.49%
Accuracy	35.94	24.32–48.90%

Table 13 ADC value less than 0.99 (our calculated cut-off value) + fatty hilum + cortical thickness > 4 mm + type II dynamic curve

Statistic	Value (%)	95% CI
Sensitivity	14.58	6.07–27.76%
Specificity	100.00	79.41–100.00%
Disease prevalence	75.00	62.60–84.98%
Positive predictive value	100.00	
Negative predictive value	28.07	25.77–30.49%
Accuracy	35.94	24.32–48.90%

Table 14 ADC value less than 0.99 (our calculated cut-off value) + fatty hilum + cortical thickness > 4 mm + type III dynamic curve

Statistic	Value (%)	95% CI
Sensitivity	16.67	7.48–30.22%
Specificity	100.00	79.41–100.00%
Disease prevalence	75.00	62.60–84.98%
Positive Predictive value	100.00	
Negative predictive value	28.57	26.06–31.22%
Accuracy	37.50	25.70–50.49%

statistically significant feature suggesting malignancy. Twenty-one (41.2%) of the metastatic lymph nodes and 31 (20.4%) of the non-metastatic lymph nodes showed eccentric cortical thickening (*p* value 0.003). In this study, cortical thickness of lymph nodes could significantly predict malignant infiltration with *p* value 0.006, using cut-off value of 4.5 mm, with a sensitivity of 68.8%, specificity of 62.5%, and diagnostic accuracy of 64.1%. A study by Fornasa et al. [17] mentioned that infiltrated lymph nodes were defined as follows: maximal cortical thickness more than 4 mm, an ADC value of $0.986 \times 10^{-3} \text{ mm}^2/\text{s}$ or lower, and abnormal shape (fatty hilum loss or eccentric cortical thickening). In our study, maximal cortical thickness more than 4.5 mm, an ADC value of $0.99 \times 10^{-3} \text{ mm}^2/\text{s}$ or lower, and abnormal shape including eccentric cortical thickening or fatty hilum loss defined infiltrated lymph nodes. In our study, a total of 23 (47.9%) out of 48 metastatic lymph nodes had eccentric/lost fatty hilum, while 100% of non-metastatic lymph nodes had intact fatty hilum. There was a statistically significant difference between eccentric and normal fatty hilum status with *p* value 0.0001, sensitivity of 47.9%, specificity of 93.7%, and diagnostic accuracy of 82.3% of eccentric hilum for detection of malignant lymph nodes. A study by Baltzer

et al. [7] stated that the use of a small ROI placed on the darkest part of the lesion on the ADC map, avoiding noisy, necrotic, or non-enhancing lesion voxels is currently recommended and that what we applied during our post-processing. A study by Fornasa et al. [17] illustrated that the ADC values of the lymph nodes with metastases (mean: $0.878 \times 10^{-3} \text{ mm}^2/\text{s}$; range: 0.30–1.20) were significantly lower ($p < 0.001$) than those of the benign lymph nodes (mean: 1.494; range: 0.60–2.50). Adopting a threshold value of $1.09 \times 10^{-3} \text{ mm}^2/\text{s}$ resulted in 94.7% sensitivity, 91.7% specificity, and 93.0% accuracy in the identification of metastasis in this series of lymph nodes. He et al. [18] reported that the mean ADC value of the metastatic lymph nodes ($0.910 \pm 0.29 \times 10^{-3} \text{ mm}^2/\text{s}$) was significantly lower than that of the non-metastatic nodes ($1.270 \pm 0.32 \times 10^{-3} \text{ mm}^2/\text{s}$). Kim et al. [9] found that the mean ADC value of the metastatic lymph nodes ($0.910 \pm 0.29 \times 10^{-3} \text{ mm}^2/\text{s}$) was significantly lower than that of the non-metastatic nodes ($1.270 \pm 0.32 \times 10^{-3} \text{ mm}^2/\text{s}$). Based on the ROC curves, the ADC value was a strong variable for predicting a metastatic node (AUC, 0.815). An ADC value of $0.986 \times 10^{-3} \text{ mm}^2/\text{s}$ was determined, with sensitivity, specificity, PPV, and NPV of 75.8%, 83.9%, 72.6%, and 86.0%, respectively. Fardanesh et al. [19] stated that the median values of mean ADC, maximum ADC, and minimum ADC were significantly lower for malignant lymph

nodes rather than benign axillary lymph nodes. In their study, the ADC values ($\times 10^{-3} \text{ mm}^2/\text{s}$) of benign axillary lymph nodes ranged from 0.52 to 2.71, while the ADC values ($\times 10^{-3} \text{ mm}^2/\text{s}$) of malignant axillary lymph nodes ranged from 0.80 to 1.08. We found that the mean ADC value of metastatic axillary LNs (0.55; range being 0.23 to $0.98 \times 10^{-3} \text{ mm}^2/\text{s}$) was lower than that of the benign ones (0.82, range from 0.34 to $1.4 \times 10^{-3} \text{ mm}^2/\text{s}$). Baltzer et al. [7] reported that the mean ADC threshold that resulted in the highest diagnostic accuracy for differentiating between benign and malignant lymph nodes was $1.004 \times 10^{-3} \text{ mm}^2/\text{s}$, yielding an accuracy of 75%, sensitivity of 71%, specificity of 79%, the PPV of 77%, and NPV of 74%. In the present study, we found that ADC value can significantly predict lymph node infiltration with p value 0.011, using a cut-off value of 0.99, with sensitivity 43.85, specificity 100%, diagnostic accuracy 57.8% and AUC 71.4%. In the current study, we found that the DCE-MRI curve was type I in 19 (29.7%) patients, type II in 27 (42.2%) patients, and type III in 18 (28.1%) patients. Comparison of pathological findings according to type of DCE-MRI curve showed that there was a statistically significant correlation between pathological findings and DCE-MRI curve type III with p value 0.0001, showing a sensitivity of 37.5%, specificity of 100%, and diagnostic accuracy of 84.4% for detection of malignant lymph nodes (Figs. 5, 6, 7, 8).

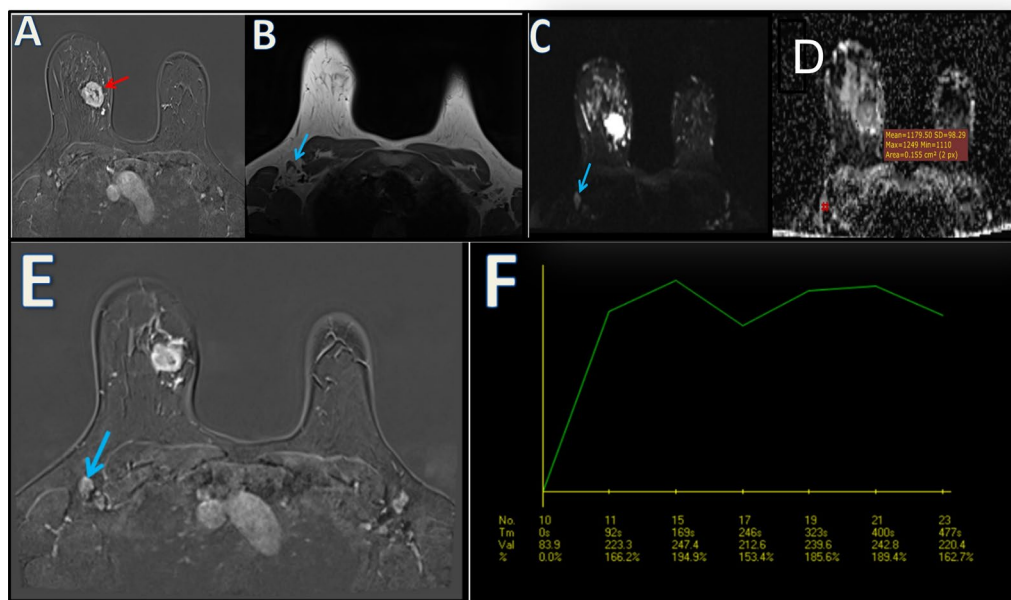


Fig. 5 A 36-year-old female with a right breast upper inner quadrant malignant mass and an ipsilateral axillary lymph node. **A** post-contrast subtraction image of the right breast lesion (red arrow), **B** T1WI of the lymph node showing focal cortical thickness reaching 7 (blue arrow). **C, D** DWI and ADC map of the lymph node showing restricted diffusion and ADC value of $1.1 \times 10^{-3} \text{ mm}^2/\text{s}$ (above the calculated cut-off value) (blue arrow). **E** Post-contrast subtraction shows marginal enhancement of the breast mass and node, **F** Post-contrast dynamic curve of the lymph node (blue arrow) Type II curve. Impression: Indeterminate lymph node. Pathology report shows no malignancy

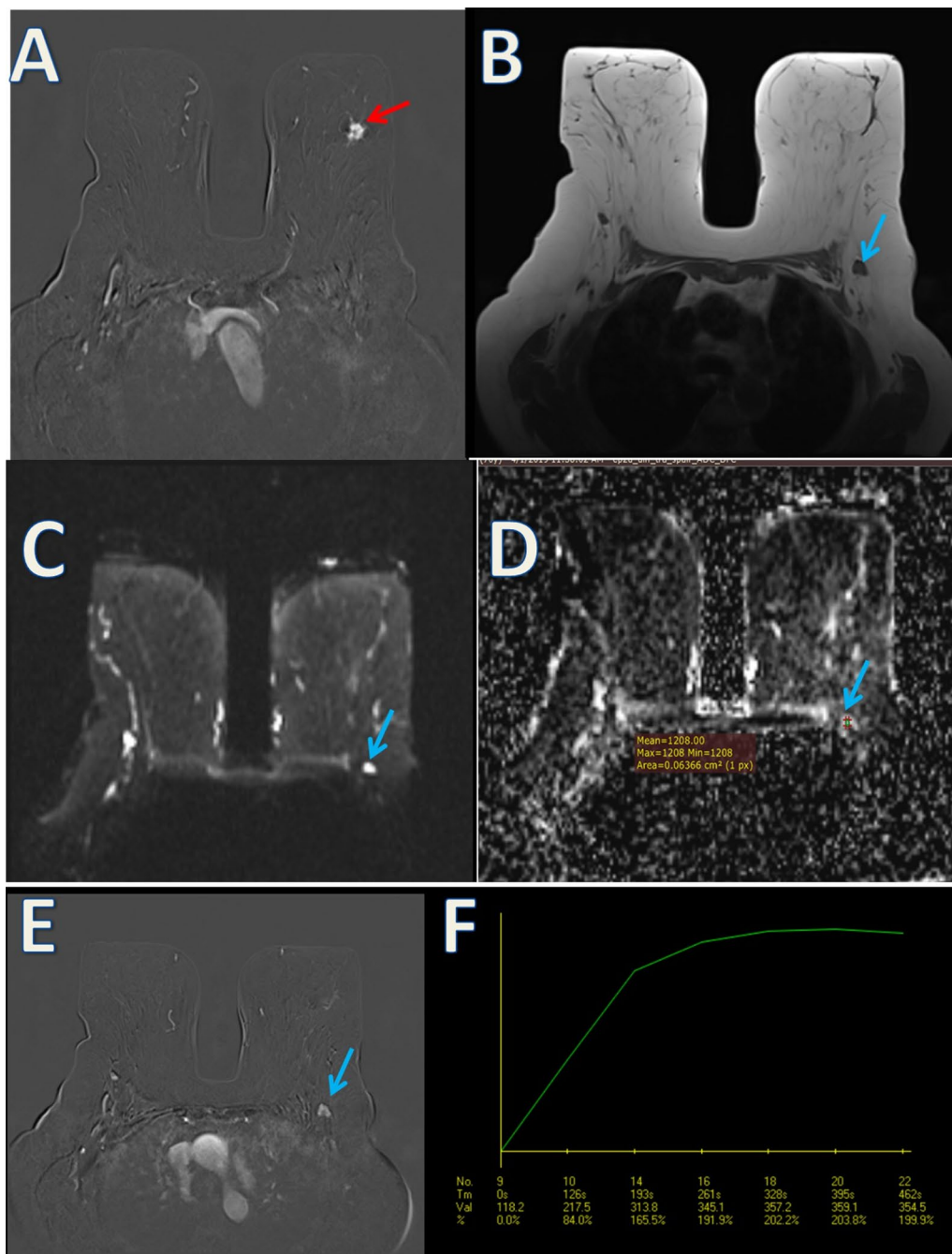


Fig. 6 A 70-year-old female with a left breast upper outer quadrant malignant mass and an ipsilateral axillary lymph node. MRI of both breasts: **A** Post-contrast subtraction image both breasts showing a spiculate intensely enhancing left breast mass. **B** T1WI of the lymph node (blue arrow) with focal cortical thickness reaching 5 mm and central fatty hilum. **C, D** DWI and ADC map shows lymph node (blue arrow) with restricted diffusion and ADC value of $1.2 \times 10^{-3} \text{ mm}^2/\text{s}$ (above calculated cut-off value). **E** Post-contrast subtraction showing the small enhancing axillary lymph node. **F** Post-contrast dynamic curve of the lymph node (blue arrow) show a type II indeterminate curve. Impression; Indeterminate lymph node. Pathology report shows no malignancy with lymphoid hyperplasia

On the contrary, Örgüç et al. [8] who studied a total of 178 lymph nodes greater than 8 mm, where 46 nodes were malignant and 132 nodes were benign, deduced that the sensitivity of type III curve was calculated as 89% as

an indicator of malignancy, yet the specificity was as low as 14%. He et al. [18] found that the shape of the time / intensity curve was type I in 29% of malignant nodes, type II in 32% of the nodes, and type III in 39% of the

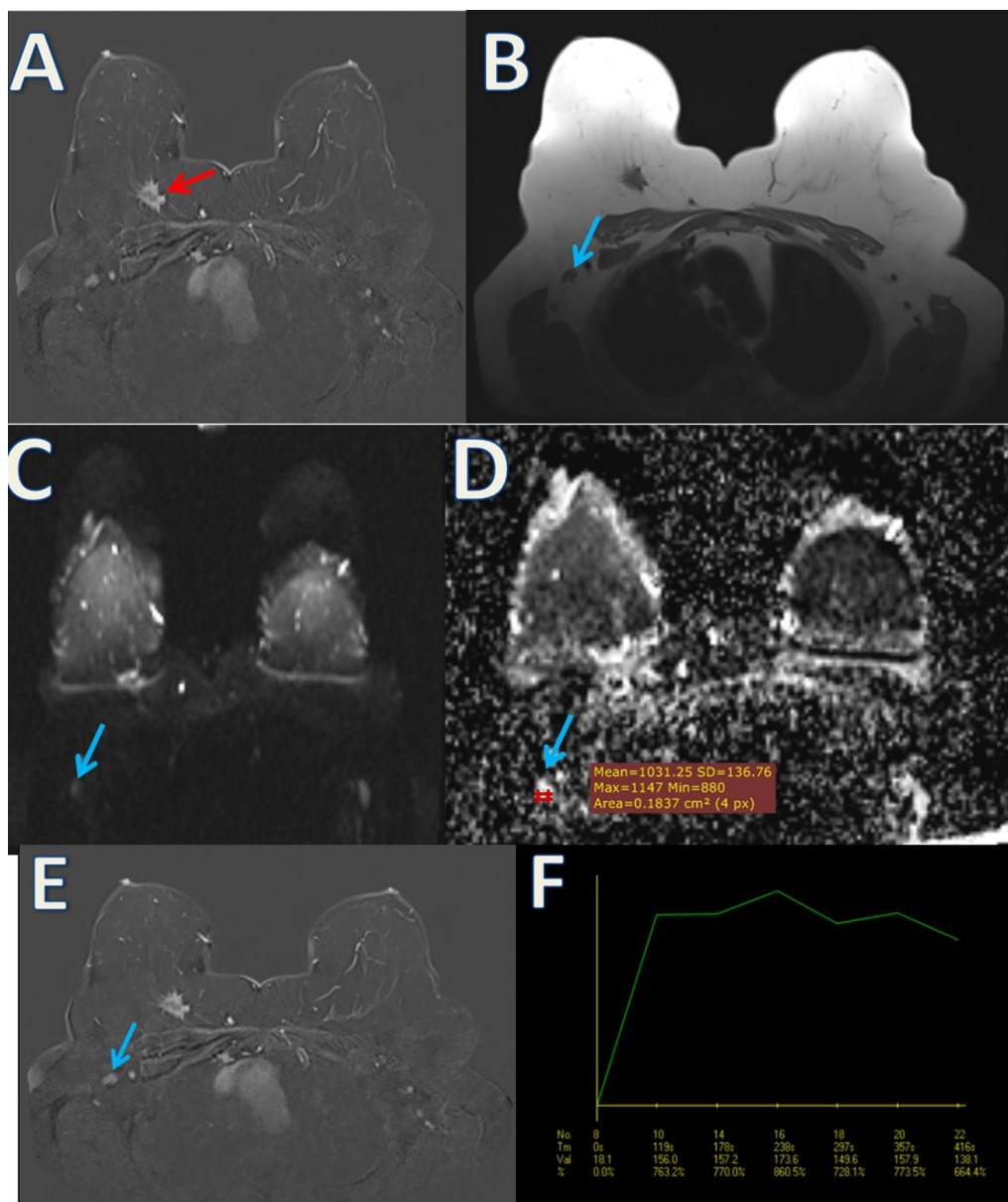


Fig. 7 A 61-year-old female with multicentric right malignant breast masses and ipsilateral axillary lymph node. MRI of both breasts: **A** post-contrast subtraction image shows a right breast mass, **B**: T1WI shows the lymph node (blue arrow) showing diffuse cortical thickness of 4 mm and central fatty hilum. **C, D** DWI and ADC map shows the lymph node with restricted diffusion and low ADC signal (ADC value of $1.0 \times 10^{-3} \text{ mm}^2/\text{s}$), (blue arrow). **E** Post-contrast subtraction showing the right breast mass and the ipsilateral axillary node, **F** post-contrast dynamic curve of the lymph node (blue arrow) showed type II (plateau) curve; Indeterminate lymph node. Pathology report shows no malignancy

nodes. Axillary lymph nodes with metastasis showed more tendency to be round or ovoid with low ADC values, $\text{ADC} \leq 1.3508 \times 10^{-3} \text{ mm}^2/\text{s}$, showing washout (type III) time/ intensity curves. Similarly, in the current study, combining ADC value less than 0.99, cortical thickness 3–4 mm, and type III dynamic curve, gave a higher diagnostic accuracy (32.81%). On the other hand, combining ADC value less than 0.99 (our calculated cut-off value),

cortical thickness >4 mm, and type III dynamic curve gave the highest diagnostic accuracy (37.50%). Limitations of this study: The small patient population included in this study may have affected the specificity and sensitivity. A wider scale research is needed to achieve higher indices. Seventy-five % of patients included in this study had malignant findings on pathological analysis; again, this might cause bias of the results. On post-processing,

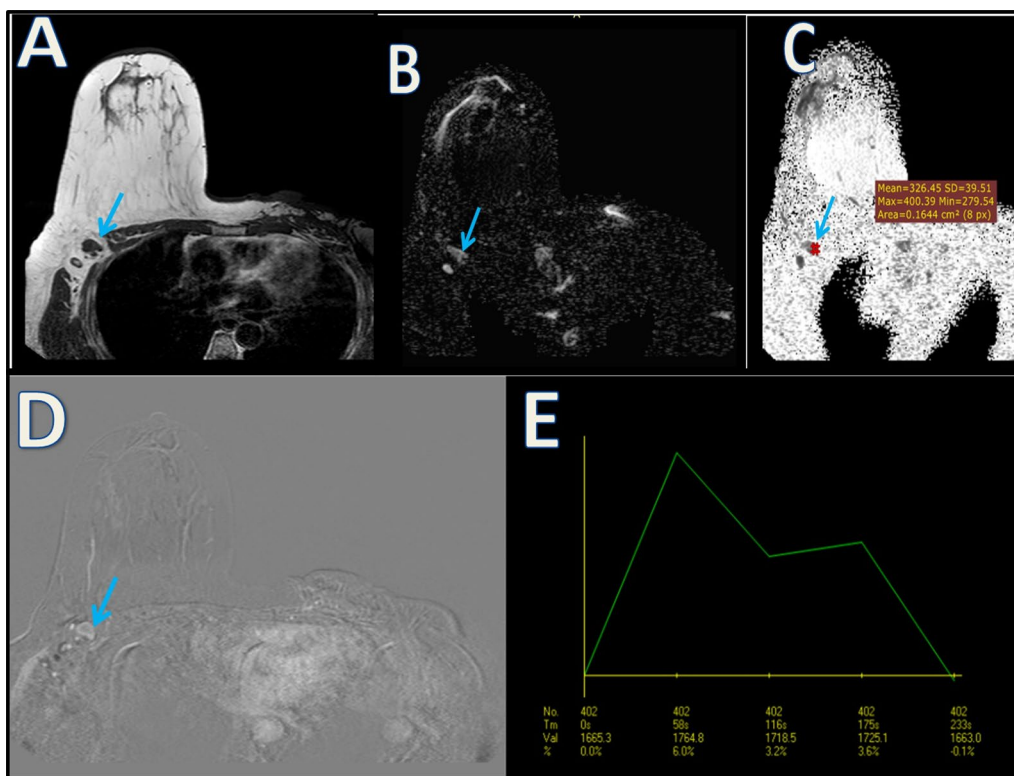


Fig. 8 A 54-year-old female who underwent left mastectomy and left axillary clearance and after 1 year she developed contralateral right indeterminate axillary lymph node MRI of both breasts: **A** T1WI showing the axillary lymph node (blue arrow). **B, C** DWI and ADC map of the lymph node which showed restricted diffusion (ADC value of $0.32 \times 10^{-3} \text{ mm}^2/\text{s}$) (blue arrow). **D** post-contrast subtraction shows that the restricted node shows marginal contrast enhancement, **E** post-contrast dynamic curve of the lymph node (blue arrow) showing type III curve; *Impression:* pathological lymph node. Pathology confirmed the malignant nature of the lymph node

the choice of ROI is subjective from one patient to the other. A more standardized method or the use of a computerized software program to find the most restricted area of a lymph node may get more accurate results and might affect the cut-off value. Further research on a larger population is mandatory to provide more data on the role of MRI in the preoperative staging of axillary lymphadenopathy.

Conclusions

In our study, cortical thickness of lymph nodes could predict malignant infiltration with a *p* value of 0.006, using cut-off value of 4.5 mm, and a diagnostic accuracy of 64.1%. Eccentric hilum of lymph nodes could also detect malignancy with a *p* value of 0.0001 and a diagnostic accuracy of 82.3%. ADC value could predict lymph node infiltration with a *p* value of 0.011, using a cut-off value of 0.99 and a diagnostic accuracy of 57.8%. DCE-MRI curve type III showed a diagnostic accuracy of 84.4% for detection of malignant lymph nodes.

Abbreviations

- ADC Apparent diffusion coefficient
- ALN Axillary lymph node
- ALND Axillary lymph node dissection
- CNB Core needle biopsy
- DCE-MRI Dynamic contrast enhanced MRI
- FNA Fine needle aspiration
- LNS Lymph nodes
- SLNB Sentinel lymph node biopsy

Acknowledgements

Thanks are due to patients and MRI applicators who contributed to this work.

Author contributions

Equal sharing in data collection and analysis, manuscript writing, and editing were done by the four authors. RH and SK did the initial manuscript writing and data analysis. FA was assigned to data collection and technique. SM shared in writing, editing, and revising data and manuscript. All authors have read and approved the final manuscript.

Funding

Self-funding.

Availability of data and materials

All data and materials used in this research are available.

Declarations

Ethics approval and consent to participate

The study protocol was approved by the Local Ethics Committee. Vancouver ethical standards were followed in the conduct of the study. This study was conducted after institutional and departmental ethical clearance and informed consent was obtained from patients or their authorized representatives. Ethics committee code: MD-94-2021.

Consent for publication

All patients included in this research gave written informed consent to publish the data contained and/or analyzed within this study.

Competing interests

The authors declare they have no competing interests.

Received: 15 April 2023 Accepted: 2 August 2023

Published online: 10 October 2023

References

- Chang JM, Leung JW, Moy L, Ha SM, Moon WK (2020) Axillary nodal evaluation in breast cancer: state of the art. *Radiology* 295(3):500–515
- Plaza MJ, Wright J, Fernandez S (2021) COVID-19 vaccine-related unilateral axillary lymphadenopathy: pattern on screening breast MRI allowing for a benign assessment. *Clin Imaging* 80:139–141
- Chung J, Youk JH, Kim JA, Gweon HM, Kim EK, Ryu YH, Son EJ (2014) Role of diffusion-weighted MRI: predicting axillary lymph node metastases in breast cancer. *Acta Radiol* 55(8):909–916
- Korteweg MA, Zwanenburg JJ, Hoogduin JM, Van Den Bosch MA, Van Diest PJ, Van Hillegersberg R, Eijkemans MJ, Mali WP, Luijten PR, Veldhuis WB (2011) Dissected sentinel lymph nodes of breast cancer patients: characterization with high-spatial-resolution 7-T MR imaging. *Radiology* 261(1):127–135
- Elmesidy DS, Badawy EA, Kamal RM, Khallaf ES, AbdelRahman RW (2021) The additive role of diffusion-weighted magnetic resonance imaging to axillary nodal status evaluation in cases of newly diagnosed breast cancer. *Egypt J Radiol Nucl Med* 52(1):1–2
- Baltzer PA, Dietzel M, Burmeister HP, Zoubi R, Gajda M, Camara O, Kaiser WA (2011) Application of MR mammography beyond local staging: is there a potential to accurately assess axillary lymph nodes? Evaluation of an extended protocol in an initial prospective study. *Am J Roentgenol* 196(5):W641–W647
- Baltzer P, Mann RM, Lima M, Sigmund EE, Clauser P, Gilbert FJ, Martincich L, Partridge SC, Patterson A, Pinker K, Thibault F, Camps-Herrero J, Le Bihan D, EUSOBI international Breast Diffusion-Weighted Imaging working group (2020) Diffusion-weighted imaging of the breast—a consensus and mission statement from the EUSOBI International Breast Diffusion-Weighted Imaging working group. *Eur Radiol* 30(3):1436–1450. <https://doi.org/10.1007/s00330-019-06510-3>
- Örgüç FF (2011) Diffusion-weighted magnetic resonance imaging: what makes water run fast or slow? *J Clin Imaging Sci* 1:27. <https://doi.org/10.4103/2156-7514.81294>
- Kim EJ, Kim SH, Kang BJ, Choi BG, Song BJ, Choi JJ (2014) Diagnostic value of breast MRI for predicting metastatic axillary lymph nodes in breast cancer patients: diffusion-weighted MRI and conventional MRI. *Magn Reson Imaging* 32(10):1230–1236
- De Camargo Teixeira PA, Chala LF, Shimizu C, Filassi JR, Maesaka JY, de Barros N (2017) Axillary lymph node sonographic features and breast tumor characteristics as predictors of malignancy: a nomogram to predict risk. *Ultrasound Med Biol* 43(9):1837–1845
- Mainiero MB, Cinelli CM, Koelliker SL, Graves TA, Chung MA (2010) Axillary ultrasound and fine-needle aspiration in the preoperative evaluation of the breast cancer patient: an algorithm based on tumor size and lymph node appearance. *Am J Roentgenol* 195(5):1261–1267
- Sung H, Ferlay J, Siegel RL, Laversanne M, Soerjomataram I, Jemal A, Bray F (2021) Global cancer statistics: GLOBOCAN estimates of incidence and mortality worldwide for 36 cancers in 185 countries. *CA Cancer J Clin* 71(3):209–249
- Brackstone M, Baldassarre FG, Perera FE, Cil T, Chavez Mac Gregor M, Dayes IS, Eisen AF (2021) Management of the axilla in early-stage breast cancer: Ontario Health (Cancer Care Ontario) and ASCO guideline. *J Clin Oncol* 39(27):3056–3082
- Chung HL, Le-Petross HT, Leung JW (2021) Imaging updates to breast cancer lymph node management. *Radiographics* 41(5):1283–1299
- Reig B, Heacock L, Lewin A, Cho N, Moy L (2020) Role of MRI to assess response to neoadjuvant therapy for breast cancer. *J Magn Reson Imaging* 52(6):1587–1606
- Barco I, Chabrera C, García-Fernández A, Fraile M, González S, Canales L, García Font M (2017) Role of axillary ultrasound, magnetic resonance imaging, and ultrasound-guided fine-needle aspiration biopsy in the pre-operative triage of breast cancer patients. *Clin Transl Oncol* 19(6):704–710
- Fornasa F, Nesoti MV, Bovo C, Bonavina MG (2012) Diffusion-weighted magnetic resonance imaging in the characterization of axillary lymph nodes in patients with breast cancer. *J Magn Reson Imaging* 36(4):858–864
- He N, Xie C, Wei W, Pan C, Wang W, Lv N, Wu P (2012) A new, preoperative, MRI-based scoring system for diagnosing malignant axillary lymph nodes in women evaluated for breast cancer. *Eur J Radiol* 81(10):2602–2612
- Fardanesh R, Thakur SB, Sevilimedu V, Horvat JV, Lo Gullo R, Reiner JS, Pinker K (2022) Differentiation between benign and metastatic breast lymph nodes using apparent diffusion coefficients. *Front Oncol* 12:502

Publisher's Note

Springer Nature remains neutral with regard to jurisdictional claims in published maps and institutional affiliations.

Submit your manuscript to a SpringerOpen® journal and benefit from:

- Convenient online submission
- Rigorous peer review
- Open access: articles freely available online
- High visibility within the field
- Retaining the copyright to your article

Submit your next manuscript at ► [springeropen.com](https://www.springeropen.com)